Published OnlineFirst January 23, 2012; DOI: 10.1158/0008-5472.CAN-11-1780

Cancer Research

Enhanced Apoptosis and Tumor Growth Suppression Elicited by Combination of MEK (Selumetinib) and mTOR Kinase Inhibitors (AZD8055)

Sarah V. Holt, Armelle Logie, Barry R. Davies, et al.

Cancer Res 2012;72:1804-1813. Published OnlineFirst January 23, 2012.

Published OnlineFirst January 23, 2012; DOI: 10.1158/0008-5472.CAN-11-1780

Therapeutics, Targets, and Chemical Biology

Cancer Research

Enhanced Apoptosis and Tumor Growth Suppression Elicited by Combination of MEK (Selumetinib) and mTOR Kinase Inhibitors (AZD8055)

Sarah V. Holt[1,2], Armelle Logie[1], Barry R. Davies[1], Denis Alferez[1], Sarah Runswick[1], Sarah Fenton[1], Christine M. Chresta[1], Yi Gu[3], Jingchuan Zhang[3], Yi-Long Wu[4], Robert W. Wilkinson[1], Sylvie M. Guichard[1], and Paul D. Smith[1]

Abstract

The mitogen-activated protein kinase (MAPK) and phosphoinositide 3-kinase/AKT signaling pathways interact at multiple nodes in cancer, including at mTOR complexes, suggesting an increased likelihood of redundancy and innate resistance to any therapeutic effects of single pathway inhibition. In this study, we investigated the therapeutic effects of combining the MAPK extracellular signal–regulated kinase (MEK)1/2 inhibitor selumetinib (AZD6244) with the dual mTORC1 and mTORC2 inhibitor (AZD8055). Concurrent dosing in nude mouse xenograft models of human lung adenocarcinoma (non–small cell lung cancers) and colorectal carcinoma was well tolerated and produced increased antitumor efficacy relative to the respective monotherapies. Pharmacodynamic analysis documented reciprocal pathway inhibition associated with increased apoptosis and Bim expression in tumor tissue from the combination group, where key genes such as *DUSP6* that are under MEK functional control were also modulated. Our work offers a strong rationale to combine selumetinib and AZD8055 in clinical trials as an attractive therapeutic strategy. *Cancer Res; 72(7); 1804–13. ©2012 AACR.*

Introduction

The mitogen-activated protein kinase (MAPK) intracellular signaling cascade comprises Ras, Raf, MAPK extracellular signal–regulated kinase (MEK), extracellular signal–regulated kinase (ERK1/2) and ribosomal S6 kinases and transmits signals from a number of stimuli including growth factors, hormones, and neurotransmitters, to many cellular functions including proliferation, differentiation, and cell-cycle progression (1). The pathway is commonly activated in human cancer through activating mutations of *BRAF* or the upstream small GTPase reticular activating system. Mutations in *KRAS* occur in 90% of pancreatic cancers, 45% of colorectal, and 20% of non–small cell lung cancers (NSCLC) with *BRAF* mutations present in approximately 20% to 60% of melanomas, 35% to 70% of papillary thyroid, and 12% of colorectal cancers (CRC; ref. 2). Consequently, members of this signaling pathway, including MEK, have been pursued as potential anticancer therapeutic targets. MEK contains 2 consensus kinase motifs which are involved in the phosphorylation of serine/threonine and tyrosine residues. Two homologs exist, MEK1 and MEK2, which have only one known substrate, ERK1/2, which has multiple downstream effectors involved in a number of cellular functions including transcription (e.g., Elk1), cell-cycle progression (e.g., Rb), and cell motility (e.g., JNK; ref. 1). p90RSK is activated by ERK1/2 and phosphorylates a number of substrates including elongation initiation factor (eIF) 4E-binding protein (4E-BP1), ribosomal protein S6 (S6), and Tuberin (TSC2), which are also downstream substrates of the AKT/mTOR pathway. Preclinical data showing sensitivity to a number of agents targeting MEK1/2 have been reported *in vitro* and *in vivo*, and clinical trials of these agents as monotherapies and in combination are ongoing (3–6).

In addition to MAPK pathway activation, dysregulation of the phosphoinositide 3-kinase (PI3K) cascade occurs in a number of human cancers. For example, in breast cancer activating mutations of the catalytic subunit of PI3K, p110-α (PIK3CA), occur in 30% of breast cancers and approximately 25% of NSCLC have lost expression of the PTEN tumor suppressor gene, whereas in ovarian cancers 3% to 8% have mutated and 27% have lost PTEN (7–9). Further down this

Authors' Affiliations: [1]Oncology iMed, AstraZeneca, Alderley Park, Macclesfield, Cheshire; [2]Clinical and Experimental Pharmacology, Paterson Institute for Cancer Research, Manchester, United Kingdom; [3]Innovation Centre China, AstraZeneca Global R&D, Shanghai; and [4]Guangdong Lung Cancer Institute, Medical Research Centre of Guangdong General Hospital & Guangdong Academy of Medical Sciences, Guangzhou, China

Enquiries with regard to AZD8055 can be sent to the following: Sylvie.Guichard@astrazeneca.com

Corresponding Author: Paul D. Smith, Oncology iMed, AstraZeneca Pharmaceuticals, Macclesfield, Cheshire SK10 4TG, United Kingdom. Phone: 44-0-1625-232890; Fax: 44-0-1625-519749; E-mail: Paul.D.Smith@astrazeneca.com; and Sarah V. Holt, Drug Discovery Unit, Paterson Institute for Cancer Research, Wilmslow Road, Manchester M20 4BX, United Kingdom. Email: sholt@picr.man.ac.uk

doi: 10.1158/0008-5472.CAN-11-1780

Published OnlineFirst January 23, 2012; DOI: 10.1158/0008-5472.CAN-11-1780

pathway, mutations in the tumor suppressor LKB1 have been associated with 30% NSCLC (10, 11). A number of molecules targeting components of the PI3K pathway are currently in clinical development (12). mTOR, a serine/theronine kinase, is a downstream effector of the pathway, although the PI3K pathway is not an exclusive activator of mTOR. The protein functions as a sensor of mitogen, energy, and nutrient levels and is a central controller of cell growth (13). Furthermore, mTOR has also been identified as a negative regulator of autophagy (13). mTOR forms 2 distinct complexes, mTORC1 (raptor, mLST8, and PRAS40), which is nutrient sensitive, and mTORC2 (rictor, SIN1, and protor) a nutrient and growth factor–sensitive complex. Inhibitors, such as rapamycin, inhibit the mTORC1 complex by blocking the phosphorylation of 2 major downstream kinases, p70S6 kinase (p70S6K) and 4E-BP1. However, preclinical data with mTOR kinase inhibitors including AZD8055 suggest that the inhibition of mTORC1 by rapamycin is only partial (14–16). Also, because of a negative feedback loop between p70S6K and the insulin-like receptor substrate-1 (IRS1), it has been shown that inhibition of mTORC1 activates AKT (17). Rapalogues have shown antitumor activity and are registered for use in a number of oncology settings, including renal cell carcinoma (18).

In tumor types in which mutations/modulations in either MAPK or PI3K pathway predominate, monotherapy can be considered and has shown to be effective (19, 20). However, a number of studies have presented findings that highlight acquired resistance after inhibition of one of these pathways alone (21). In addition, a number of reports have shown the presence of feedback loops that promote activity of the pathway upstream of the inhibition site. For example, rapamycin has been shown to induce the phosphorylation of AKT and eIF4E, which was overcome by the addition of the PI3K inhibitor LY294002 (22). Furthermore, another study showed enhanced MAPK pathway signaling in a PI3K-dependent feedback loop when TORC1 inhibitors were administered. Subsequently this was shown to be overcome when the MAPK pathway was inhibited (23). It has also been observed that inhibition of the MAPK pathway results in upregulation of the PI3K pathway (24). In all of these situations coadministration of inhibitors from both pathways was able to overcome the negative feedback and enhance antitumor efficacy in cell lines and/or xenograft models (25–27). Taken together, these observations suggest that in some settings suppression of one pathway alone may not be sufficient (28–30).

In this article we investigate the preclinical efficacy of a novel combination of selumetinib (AZD6244) a potent, selective, and ATP-uncompetitive inhibitor of MEK1/2 currently in phase II clinical trials (19, 31, 32) and AZD8055, a recently described (14), potent specific inhibitor of mTORC1 and mTORC2 kinase currently in phase I clinical trials. Here, we present evidence that combining these 2 inhibitors in human tumor NSCLC and CRC cell–derived xenograft and primary patient explant models shows enhanced antitumor activity. Furthermore, we present pharmacodynamic data from our *in vivo* studies showing inhibition of the PI3K and MAPK pathways and induction of apoptosis when the 2 agents are combined.

Materials and Methods

Chemicals

Selumetinib and AZD8055 were prepared as previously reported (14, 33).

Cell culture

All cell lines, including those used in human tumor xenograft studies, were cultured and assayed in Dulbecco's modified Eagle's medium (phenol red free) or RPMI 1640 + 10% fetal calf serum + 1% glutamine. All cell lines were obtained from the American Type Culture Collection and no further characterization was done.

Cell line xenografts

Female nude mice (*nu/nu:Alpk*; AstraZeneca) were housed in negative pressure isolators (PFI Systems Ltd.). Experiments were conducted in 8- to 12-week-old animals in full accordance with the United Kingdom Home Office Animal (Scientific Procedures) Act 1986. Human tumor xenografts were established by subcutaneous injection of 1×10^7, 5×10^6, 1×10^6, 1×10^7, 2.5×10^6, and 1×10^6 cells per mouse for HCT-116, A549, CaLu-6, LoVo, NCI-H2122, and NCI-H460, respectively. Animals were randomized into treatment groups ($n = 12$–14 in vehicle control group, $n = 8$–12 in treated groups) when tumors reached a defined palpable size (0.2 cm^3). Selumetinib and AZD8055 were administered by oral gavage (0.1 mL/10g). The control group received both vehicles. In the combination group, selumetinib was administered 2 hours before AZD8055. Tumor volume (measured by calipers), animal body weight, and tumor condition were recorded twice weekly during the study.

Pharmacodynamic sampling

At a defined time point selected mice were humanely culled tumors excised and cut into 2 pieces; one half was snap frozen in liquid nitrogen, whereas the other was fixed in 10% formalin buffer for 24 hours and embedded in paraffin for immunohistochemical (IHC) staining.

Immunoblotting

Protein lysate preparation and immunoblotting was done as previously described (34). Immunoblots were stained with anti-Bim (1:1,000; Chemicon), PARP (1:1,000; Cell Signaling Technology), total MAPK (1:1,000; Cell signalling Technology), phospho MAPK (Thr202/Tyr204; 1:1,000; Cell Signaling Technology), total S6 (1:1000; Cell signalling Technology), pS6 (Ser235/236; 1:1,000; Cell signalling Technology), total 4EBP-1 (1:1,000; Cell signalling Technology), phospho 4E-BP-1 (35/46; 1:1,000; Cell signalling Technology), and glyceraldehyde-3-phosphate dehydrogenase (GAPDH, 1:2,000; Abcam).

Meso scale discovery protein analysis platform

Protein lysate (0.5 mg/mL) was added per well of the MSD plate and each sample was run in duplicate. Assays were carried out and results calculated as per the manufacturers instructions (MSD) for phospho (473)/total Akt (K11100D) and analyzed on a SECTOR Imager 6000 (MSD). Results are presented as a ratio of phospho to total protein.

Published OnlineFirst January 23, 2012; DOI: 10.1158/0008-5472.CAN-11-1780

Immunocytochemistry

Tissues were processed for immunohistochemistry, stained for cleaved caspase 3, and levels of this marker were quantitated as previously described (35).

Results

Combining selumetinib and AZD8055 leads to enhanced antitumor efficacy in KRAS mutant human NSCLC xenograft models

To test the efficacy of combining selumetinib and AZD8055 *in vivo*, we selected a panel of KRAS mutant NSCLC human tumor xenograft models. The panel included models that displayed exquisite monotherapy sensitivity to selumetinib (CaLu-6) or AZD8055 (A549 Fig. 1A and Table 1). The combination of selumetinib and AZD8055 significantly enhanced antitumor efficacy in both models compared with monotherapies ($P < 0.0005$ in all cases for both models, except AZD8055 Vs combination in the A549 model $P < 0.005$). In the CaLu-6 and A549 models, the combination efficacy resulted in tumor regressions with tumor growth inhibitions (TGI) of 110% ($P < 0.0005$) and 112% ($P < 0.0005$), respectively, compared with the vehicle-treated group. Two further NSCLC models, NCI-H2122 and NCI-H460, showed an enhanced antitumor activity when exposed to the combination of selumetinib and AZD8055 compared with monotherapies alone ($P < 0.005$ for both models when the combination group was compared with either monotherapy; Table 1).

Combining selumetinib and AZD8055 inhibits the MAPK and AKT/mTOR signaling in the CaLu-6 xenografts

To investigate the pharmacodynamic effect of combining selumetinib and AZD8055 *in vivo*, animals bearing CaLu-6 tumors were exposed to an acute dosing schedule (one day of dosing) of either vehicle, monotherapy agents, or the combination schedule. Tumor lysates were assessed for expression of downstream pathway biomarkers of the MEK1/2 and AKT/mTOR pathways. In tumors treated with selumetinib alone a lower ratio of phospho to total proteins was observed for pERK1/2 (16%; $P < 0.0005$), pS6 (46%; $P < 0.0005$), and p4E-BP1 (48%; $P < 0.005$) compared with the vehicle-treated controls (Fig. 1B). Interestingly, selumetinib alone resulted in a small increase in pAKT (119%; $P < 0.05$) in CaLu-6 tumors, and

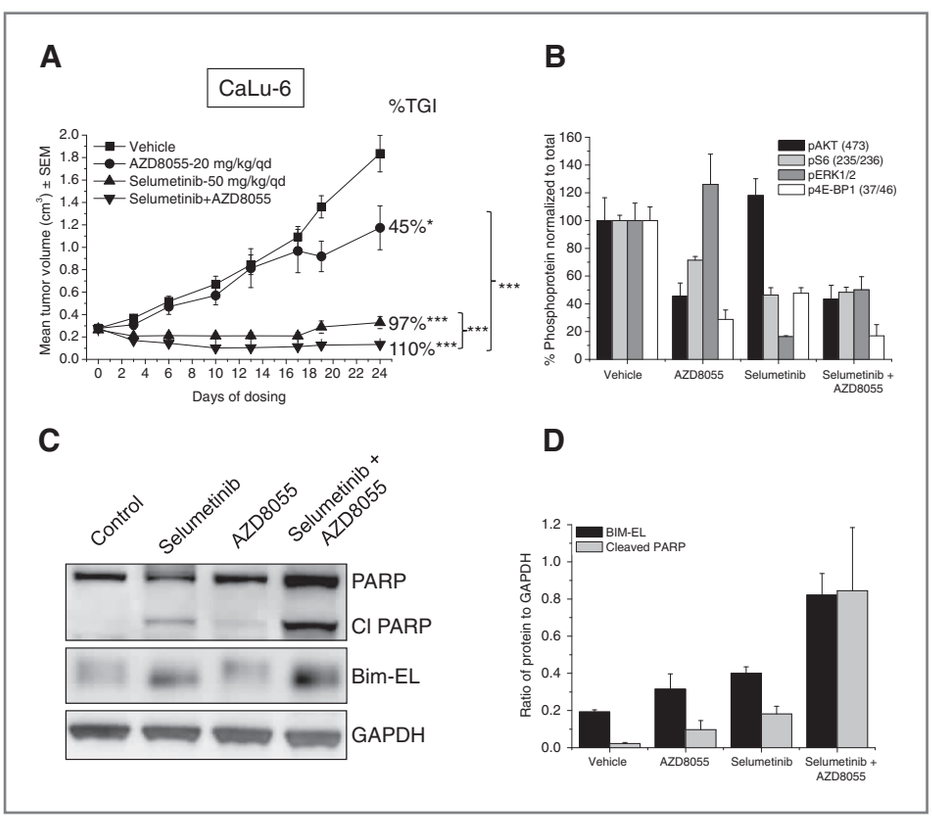

Figure 1. *In vivo* activity and pharmacodynamic response of selumetinib combined in concurrent combination with AZD8055 in the CaLu-6 NSCLC human tumor xenograft model. A, TGI in CaLu-6 tumor-bearing female nude mice when treated with either vehicle, selumetinib (50 mg/kg every day) alone, AZD8055 (20 mg/kg every day) alone, or selumetinib (50 mg/kg every day) plus AZD8055 (20 mg/kg every day) for 24 consecutive days. Percentages are expressed compared with the vehicle-treated group at the end of the dosing period. B, following one acute dose of compounds, tumor tissue was harvested 6 hours post selumetinib or 4 hours post AZD8055 and samples analyzed for pAKT(473) by mesoscale, pS6(235/236), p4EBP1(35/46), and pERK1/2 by Western blotting followed by densitometry analysis and presented in a ratio of phospho:total protein, all data presented as a % of the control. C, Western blot analysis of Bim-EL and cleaved PARP showing GAPDH as a loading control and (D) quantitative densitometry analysis of Bim-EL and cleaved PARP are presented in a ratio to GAPDH. All error bars are ± SEM. *, $P < 0.05$; ***, $P < 0.0005$.

Published OnlineFirst January 23, 2012; DOI: 10.1158/0008-5472.CAN-11-1780

Table 1. Overview of selumetinib and AZD8055 combination efficacy in NSCLC human tumor xenograft and primary tumor explant models

Model	Xenograft or patient-derived explant	Mutation status	Selumetinib (mg/kg every day)	Selumetinib (%TGI)	AZD8055 (mg/kg every day)	AZD8055 (%TGI)	Selumetinib + AZD8055 (%TGI)
CaLu-6	Xenograft	KRAS	50	97[a]	20	45[b]	110[a]
A549	Xenograft	KRAS/LKB	25	53[a]	20	85[a]	112[a]
NCI-H2122	Xenograft	KRAS/LKB	50	34[c]	20	54[a]	96[a]
NCI-H460	Xenograft	KRAS/LKB/PIK3CA	50	26[a]	20	64[a]	77[a]
L004	Explant	KRAS WT/EGFR WT	25	48[c]	20	87[a]	113[a]

NOTE: %TGIs are expressed compared with the vehicle-treated group.
[a]$P < 0.0005$
[b]$P < 0.05$
[c]$P < 0.005$

this was also observed in HCT-116 xenografts (Figs. 1B and 2B) and has been previously reported in studies using MEK1/2 inhibitors (36, 37). Tumors exposed to AZD8055 alone showed lower expression of pAKT (45%; $P < 0.05$), pS6 (71%; $P < 0.005$), and p4E-BP1 (28%; $P < 0.005$) compared with the vehicle-treated group (Fig. 1B). AZD8055, whether as a single agent or in combination with selumetinib, caused an increase in pERK1/2 levels compared with vehicle or selumetinib alone, respectively. This is probably because of inhibition of PI3K signaling pathway leading to a release of negative feedback on the MAPK pathway as previously reported (21). When selumetinib and AZD8055 were combined, the levels of pERK1/2 and pAKT were observed to decrease compared with vehicle-treated tumors (Fig. 1B), suggesting that downstream markers for either pathway can be inhibited simultaneously in the CaLu-6 xenograft model. Interestingly, lower levels of 4E-BP1 were seen in the combination-treated tumors (16.9%) compared with monotherapies (47.7% in selumetinib and 28.7% in AZD8055); however, this was not statistically significant.

Selumetinib combined with AZD8055 induced apoptosis in CaLu-6 xenografts

In view of the enhanced regression seen in the combination-treated tumors, we investigated the expression of apoptotic biomarkers in the tumors following treatments. In both the selumetinib and AZD8055 monotherapy groups there was an increase in the level of cleaved PARP compared with the vehicle-treated group ($P > 0.05$ for AZD8055 and was not significant; Fig. 1C and D). However, in tumor tissue taken from animals dosed with the combination of selumetinib and AZD8055, an increase in cleaved PARP was observed that was greater than that in either monotherapy group (Fig. 1C and D). In addition, in tumors treated with selumetinib or AZD8055 alone, a small increase in Bim-EL compared with the vehicle group was observed ($P > 0.05$ for AZD8055 and was not significant; Fig. 1C and D). In tumors that had received the combination of both agents, an increase of Bim-EL was shown to be approximately 4-fold and approximately 2-fold greater than the vehicle- and monotherapy-treated groups, respectively. Furthermore, a phosphorylation shift was observed in the control- and AZD8055-treated tumors, but this was not observed in the selumetinib and combination groups consistent with published observations that activation of Erk1/2 promotes Bim phosphorylation (refs. 38, 39; Fig. 1C).

Combination of selumetinib and AZD8055 in KRAS mutant colorectal xenografts

To determine the utility of combining selumetinib and AZD8055 in other types of cancer we investigated the effect of the combination in KRAS mutant human CRC xenograft models (LoVo and HCT-116). In LoVo xenografts the combination of selumetinib and AZD8055 resulted in a 93% ($P < 0.0005$) TGI compared with 43% ($P < 0.0005$) for selumetinib and 66% ($P < 0.0005$) in AZD8055-treated tumors (Table 2). In HCT-116 xenografts, selumetinib and AZD8055 as monotherapies showed enhanced TGI compared with the control of 59% ($P < 0.0005$) and 24% ($P < 0.05$), respectively (Fig. 2A). In combination the compounds resulted in a TGI of 89% ($P < 0.0005$) compared with the vehicle-treated group. Statistical analysis showed that there was a significant difference between the efficacies observed in the monotherapy verses the combination groups.

Pharmacodynamic analysis of combining selumetinib and AZD8055 in HCT116 xenografts

After a chronic dosing schedule (14 doses) tumor tissue from HCT116 xenografts treated with vehicle, monotherapies, or the combination of both compounds was processed and levels of the primary biomarkers pERK1/2, pAKT, and pS6 were assessed. In tumors from animals dosed with selumetinib a reduction in pERK1/2 (21%) and pS6 (43%) were observed (Fig. 2B). AZD8055 alone resulted in lower levels of pAKT (41%) and pS6 (36%). In tumors from animals that had received the concurrent combination of selumetinib and AZD8055, levels of all key biomarkers were lower compared with the vehicle-treated control pERK1/2 (21%), pS6 (6%), and pAKT (43%; Fig. 2B). Interestingly, the reduction in pS6 in the combination

Published OnlineFirst January 23, 2012; DOI: 10.1158/0008-5472.CAN-11-1780

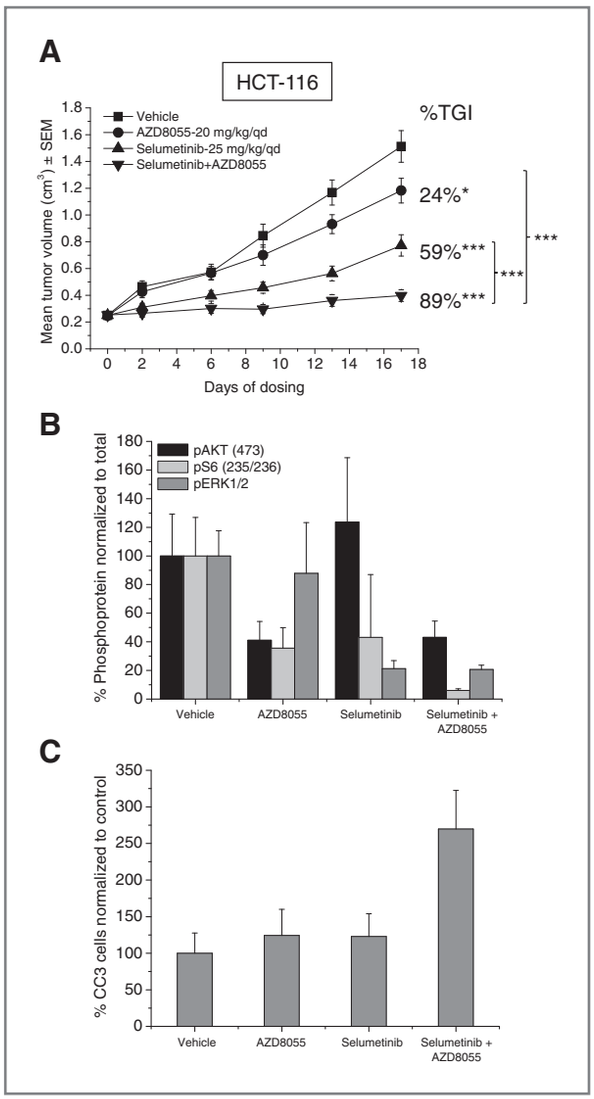

Figure 2. Concurrent combination of selumetinib and AZD8055 in the HCT-116 colorectal xenograft model. A, TGI in HCT-116 tumor-bearing female nude mice treated with either vehicle, selumetinib alone, AZD8055 alone, or selumetinib plus AZD8055 daily for 17 consecutive days. Percentages are expressed compared with the vehicle-treated group at the end of the dosing period. Statistical comparison between the monotherapy and combination groups was done using a one-tailed *t* test. B, after a chronic dosing schedule (14 doses), tumor tissue was collected 8 hours post selumetinib or 6 hours post AZD8055. Tumor tissue was processed and quantitative analysis for pAKT(473) by mesoscale, pS6 (235/236), and pERK1/2 by Western blotting was carried out. All phospho levels were normalized to total protein and presented as a% of the control. C, quantitative analysis of cleaved caspase 3 immunohistochemistry was done by Chroma Vision and results are presented as a % of the vehicle-treated group. All error bars are ± SEM. *, $P < 0.05$; ***, $P < 0.0005$.

group was greater than that in the either monotherapy group although this was not significant.

To assess the mechanism of interaction between selumetinib and AZD8055 IHC analysis was done on the tumor tissue to assess levels of the apoptotic marker cleaved caspase 3. Quantitative analysis did not show an increase in this marker in selumetinib or AZD8055 monotherapy groups compared with the vehicle (Fig. 2C). However, when the 2 compounds were combined an increase in cleaved caspase 3 of approximately 150% ($P < 0.05$) compared with the monotherapy groups was observed. Taken together the data presented here suggest that combined inhibition of the MEK and mTOR pathways results in enhanced antitumor efficacy due to an increase in apoptosis.

Concurrent combination of selumetinib and AZD8055 in a KRAS wild-type patient-derived NSCLC xenograft model shows antitumor efficacy and apoptosis

We then investigated whether the enhanced efficacy of the selumetinib/AZD8055 combination was seen in a model without a *KRAS* mutation. To test this we used a patient-derived NSCLC xenograft model, L004, which is wild-type for KRAS and EGFR. Selumetinib and AZD8055 were administered daily following the same study protocol as described previously. After 20 days of dosing, TGI was 48% ($P < 0.005$) and 87% ($P < 0.0005$) in response to selumetinib and AZD8055, respectively (Fig. 3A). In the combination group TGI was observed to be 113% ($P < 0.0005$), suggesting tumor regression compared with the vehicle-treated animals. Statistical analysis showed a significant difference between the monotherapy groups and the combination.

The effect of combining selumetinib and AZD8055 in the L004 KRAS wild-type model was investigated pharmacodynamically. In tumors exposed to selumetinib alone, levels of pERK1/2 were reduced to 22% compared with the vehicle-treated group. Furthermore, lower levels of pS6 (65%), p4E-BP1 (69%), and pAKT (85%) were observed. When mTOR was inhibited by AZD8055 reduction in levels of pAKT (19%), pS6 (14%), and p4E-BP1 (17%) were observed compared with the vehicle. Interestingly, as seen in the CaLu-6 model in xenograft tissue from animals treated with AZD8055, pERK1/2 levels were observed to be increased to 174% compared with the vehicle-treated tissues. However, this was not observed in the combination group as pERK1/2 levels were reduced to 42% compared with the vehicle, suggesting that inhibition of the MEK pathway by selumetinib had repressed the upregulation observed in xenograft tissue from animals treated with AZD8055. The combination enhanced suppression of pS6 (6%) and p4E-BP1(7%) levels compared with monotherapies, as previously observed in the CaLu-6 model.

To investigate the potential mechanism of action when selumetinib and AZD8055 were combined in this model, levels of the apoptotic markers, cleaved PARP, and Bim were analyzed and showed enhanced levels in the combination group compared with the vehicle- and monotherapy-treated groups (Fig. 3C).

Selumetinib combined with AZD8055 results in enhanced antitumor efficacy in patient-derived colorectal xenograft explants

Previous analysis of patient-derived xenografts has indicated that, in comparison with cell lines derived xenografts, they exhibit a more complex histopathologic morphology (e.g., hypovascular, varying degrees of dysplasia) and offer greater

Published OnlineFirst January 23, 2012; DOI: 10.1158/0008-5472.CAN-11-1780

Table 2. Overview of selumetinib and AZD8055 combination efficacy in CRC human tumor xenograft and primary tumor explant models

Model	Xenograft or patient-derived explant	Mutations	Selumetinib (mg/kg every day)	Selumetinib (%TGI)	AZD8055 (mg/kg every day)	AZD8055 (%TGI)	Selumetinib + AZD8055 (%TGI)
HCT-116	Xenograft	KRAS/PIK3CA	25	59[a]	20	24[b]	89[a]
LoVo	Xenograft	KRAS/PIK3CA/APC	50	43[a]	20	66[a]	93[a]
TC-305	Explant	KRAS/PIK3CA/p53/APC	25	50[a]	10	32[b]	73[a]
TC-71	Explant	KRAS/PTEN/p53/APC	25	41[c]	10	41[c]	73[a]
TC-302	Explant	KRAS/p53/APC	25	58[a]	40	35[b]	89[a]

NOTE: %TGIs are expressed compared with the vehicle-treated group.
[a]$P < 0.0005$
[b]$P < 0.05$
[c]$P < 0.005$

genetic diversity and therefore may represent better models of clinical disease (40). Therefore to investigate further the effects of selumetinib and AZD8055 we conducted combination therapy in 3 CRC explants, chosen because of their varied morphology and genetics.

In the TC-305 model animals were exposed to 25 mg/kg selumetinib and/or 10 mg/kg AZD8055. As monotherapies selumetinib and AZD8055 showed antitumor efficacy of 32% ($P < 0.05$) and 50% ($P < 0.0005$), respectively, compared with the vehicle-treated group. When both agents were administered in concurrent combination, there was a significant enhancement of antitumor efficacy of 73% ($P < 0.0005$; Fig. 4 and Table 2). Statistical analysis showed presence of a significant difference between the monotherapy and combination groups. The combination efficacy was also observed in 2 other CRC explant models TC-71 and TC-302 (Table 2), in which monotherapies had a moderate effect on antitumor activity.

Gene expression profiling of xenografts exposed to selumetinib and AZD8055

To build on our understanding about the effect of combining selumetinib and AZD8055 on proximal and phenotypic biomarkers, we wanted to determine whether inhibiting these pathways in combination correlated with functional transcriptional pathway outputs. Gene expression analysis by real-time quantitative reverse transcriptase PCR for an 18-gene signature, which has been reported to identify MEK functional output independent of tumor type (41), was done on xenograft tissue following exposure to the combination or monotherapy agents in 3 of our xenograft models (CaLu-6, HCT-116, and LoVo).

Several genes, which had a P value less than 0.05 and a fold change of at least 1.4, in all 3 xenograft models tested decreased in response to selumetinib, compared with vehicle, (DUSP4, DUSP6, and ETV4; Fig. 5). Other genes were modulated in at least 2 of the models (ETV5, MAP2K3, SLCO4A1, and SPRY2), or in the CaLu-6 (LZTS1, PHLDA1, and TRIB2), or the HCT-116 (SERPINB1) models alone. Tumors exposed to AZD8055 did not seem to have a significant effect on the gene signature apart from DUSP4, which increased ($P < 0.05$ and more than 1.4-fold change) in response to mTOR inhibition in the CaLu-6 and HCT-116 models. In addition, an increase in dual-specificity phosphatase 6 (DUSP6; $P < 0.05$ and more than 1.4-fold change) and SLCO4A1 ($P < 0.05$ and more than 1.4-fold change) and a decrease in LZTS1 ($P < 0.05$ and more than 1.4-fold change) was observed in HCT-116 xenografts. The general observation in the combination groups was that similar gene changes were seen to those of the selumetinib monotherapy indicating that AZD8055 was not adding to or inhibiting the functional output from selumetinib.

Discussion

In recent years numerous agents targeting the Ras/Raf/MEK or PI3K/AKT/mTOR pathways have entered clinical development, and dual targeting of these pathways is now been investigated clinically. It had been generally accepted, and shown, that direct inhibition of targets subject to mutational activation is effective (42), and this expectation has to some extent translated to cases in which the mutationally activated pathway is targeted at a nonmutated node (e.g., MEK inhibitors and Rapalogues). However, in some settings these initial observations have been shown to be more complicated, and the dependency of cancer cells for survival on both of these pathways is becoming better understood (25, 27, 43). In this study we report that dual targeting of the MEK and mTOR pathways, using well-tolerated schedules of the inhibitors selumetinib and AZD8055, respectively, results in enhanced antitumor efficacy across a panel of NSCLC and CRC xenograft and patient-derived explant models. Furthermore, pharmacodynamic analysis of tumor tissue taken from several of these studies showed MAPK and mTOR pathway suppression, enhanced apoptotic signaling, and the modulation of MEK functional output pathways following exposure to both agents.

Our initial investigations determined the efficacy of combining selumetinib and AZD8055 across a panel of NSCLC and CRC human tumor xenograft and explant models. There was a consistent observation that combining selumetinib and

Published OnlineFirst January 23, 2012; DOI: 10.1158/0008-5472.CAN-11-1780

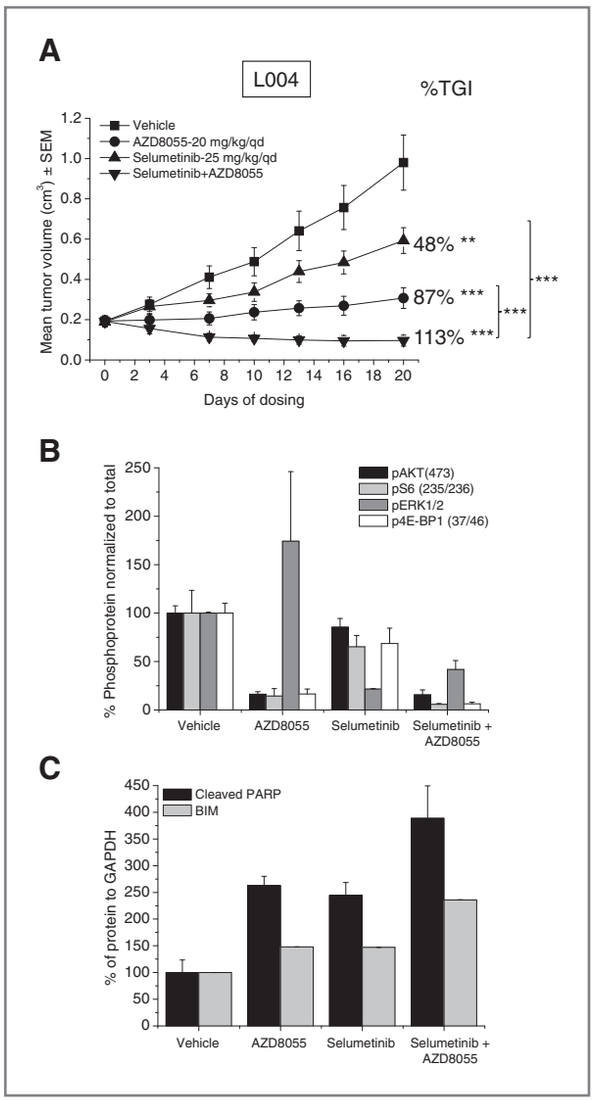

Figure 3. Concurrent combination of selumetinib and AZD8055 in a KRAS WT NSCLC primary explant model. A, TGI in L004 explant tumor-bearing female nude mice were treated with either vehicle, selumetinib alone, AZD8055 alone, or selumetinib plus AZD8055 daily for 20 consecutive days. Percentages are expressed compared with the vehicle-treated group at the end of the dosing period (%TGI). Statistical comparison between the monotherapy and combination groups was done using a one-tailed *t* test. B, following one acute dose of compounds, tumor tissue was collected 6 hours post selumetinib or 4 hours post AZD8055 and processed to analyze pAKT(473), pS6(235/236), p4EBP1(35/46), and pERK1/2 by Western blotting followed by densitometry analysis. All phospho levels were normalized to total protein and presented as a % of the control. C, cleaved PARP and Bim normalized to GAPDH was analyzed by Western blot and quantitation done by densitometry. All error bars are ± SEM. **, $P < 0.005$; ***, $P < 0.0005$.

AZD8055 was more efficacious than either agent alone in any of the xenograft or explant models tested here. A large proportion of the models we used had a *KRAS* mutation as this occurs in approximately 20% and 45% of NSCLC and CRC, respectively (2). However, some of these cell lines also harbor other mutations such as *LKB1* and *PIK3CA* and were therefore not all exquisitely sensitive to selumetinib (Tables 1 and 2). We also tested the combination in a KRAS wild-type setting, the L004 NSCLC explant model, which showed the significant beneficial effects of the combination (Fig. 3). We explored a wide variety of models with differing genetic backgrounds and monotherapy response rates to try and understand the dependency of the combination on cellular pathway signaling and potential escape routes and feedback mechanisms (24, 44, 45). A recent study highlighted the issue of feedback loops between the MAPK and PI3K pathways following a prolonged exposure to single agents targeting either pathway alone (21). This article described that in RTK-activated or *KRAS* mutant cell lines, when inhibitors specific for the individual pathways were administered in combination, the reciprocal pathway activation was overcome and resulted in an increase in apoptosis and tumor shrinkage in xenograft models. Given the existence and complexity of mutations to these 2 pathways, it has been suggested that in some cases combined inhibition of both pathways maybe required to restore sensitivity to MEK inhibition, such as that shown when *PIK3CA* mutations were ablated (28). Investigations into the exposure of transgenic mice harboring murine lung cancers with either *PIK3CA H1047R* or *KRAS G12D* mutations to the PI3K/mTOR agent NVP-BEZ235 showed that as a monotherapy the agent was effective in PIK3CA mutant lung cancers, but not against *KRAS* mutations (25). However, when combined with selumetinib, NVP-BEZ235 was more effective than either agent alone.

As part of our pharmacodynamic studies, we observed in several models a small, although not statistically significant ($P < 0.05$), increase in pAKT in response to MEK inhibition with selumetinib, an observation which has also been recently reported in melanoma cell lines (36). Consistent with our findings Gopal and colleagues showed that inhibition of AKT,

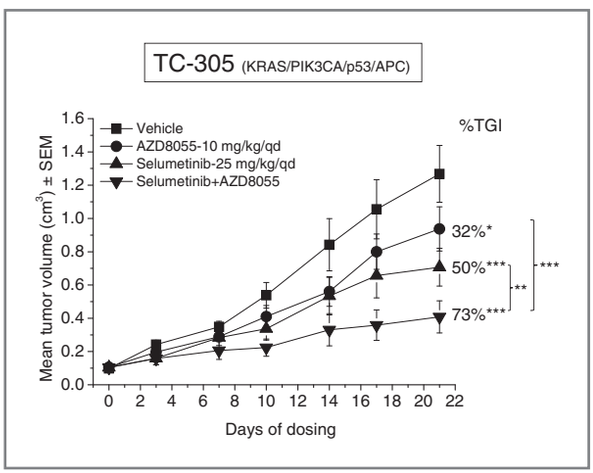

Figure 4. Selumetinib combined with AZD8055 results in enhanced antitumor efficacy in a patient-derived colorectal explant model. TGI in TC-305 tumor-bearing male nude mice was treated with either vehicle, selumetinib alone, AZD8055 alone, or selumetinib plus AZD8055 concomitantly. Percentages are expressed compared with the vehicle-treated group at the end of the dosing period (%TGI). Statistical comparison between the monotherapy and combination groups was done using a one-tailed *t* test. All error bars are ± SEM. *, $P < 0.05$; **, $P < 0.005$; ***, $P < 0.0005$.

Published OnlineFirst January 23, 2012; DOI: 10.1158/0008-5472.CAN-11-1780

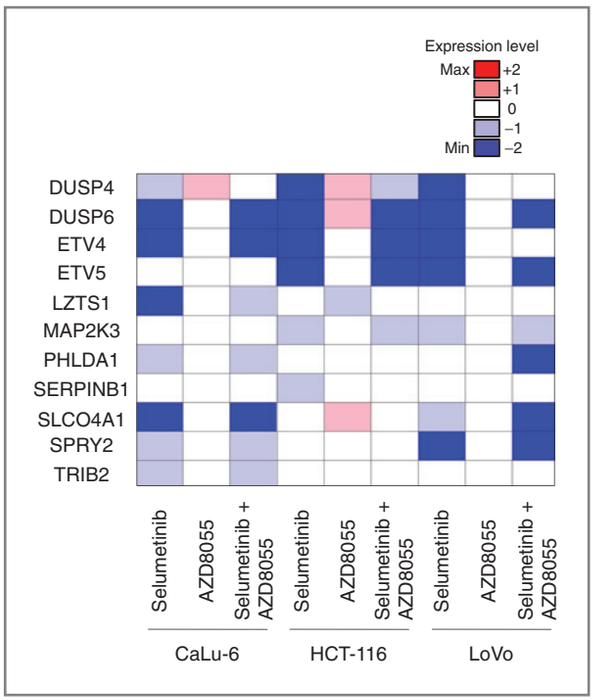

Figure 5. Heatmap showing the genes from the MEK activation signature for tissue extracted from FFPE sections for CaLu-6, HCT-116, and LoVo xenograft tissues. The CaLu-6 and HCT-116 samples were from the same tumors analyzed in Figs. 1 and 2, respectively, and LoVo samples were taken from tissues 4 hours post selumetinib or 2 hours post AZD8055 following a 5-day dosing schedule. The heatmap details of those genes in which levels changed significantly ($P < 0.05$) with a more than 1.4-fold change in response to selumetinib and/or AZD8055 compared with vehicle-treated control. Dark red boxes indicate an increase in expression with more than 2-fold change, light red boxes an increase in expression with more than 1.4-fold change, white boxes are no change compared with the vehicle-treated group, light blue boxes a decrease in expression with more than 1.4-fold change, and dark blue a decrease in expression with more than 2-fold change compared with the vehicle-treated group.

including the use of AZD8055, in combination with selumetinib was able to induce synergistic cell killing. Interestingly this was not observed when selumetinib was combined with the mTORC1 targeting agent rapamycin. This is likely to be because rapamycin, unlike AZD8055, does not inhibit the mTORC2 feedback loop and consequently AKT will still be phosphorylated and the pathway active and/or that only a partial inhibition of mTORC1 is achieved.

Inhibition of mTORC2 leads to dephosphorylation of AKT (473) and a rapid, yet transient, inhibition of AKT phosphorylation (308; ref. 46). A recent report has described an observation that mTOR inhibition, by AZD8055, relieves feedback inhibition of RTKs resulting in PI3K activation and subsequent rephosphorylation of AKT (308) which is sufficient enough to reactivate AKT activity and signaling (47). In human tumor xenograft models this observation is only made when AZD8055 was administered at doses greater than 50 mg/kg every day. In context, the work presented here uses doses that do not exceed 20 mg/kg every day. This dosing regime was well tolerated in mice and translates clinically to the equivalent maximum-tolerated dose of 90 mg twice daily, which has recently been reported for AZD8055 (48). Furthermore, we have addressed the notion that chronic administration is required to see these feedback effects (see HCT116 pharmacodynamic data Fig. 2B); we do not see a recovery of the AKT (473) signal to control values in the AZD8055-treated group. It is also possible that apparent differences between our data and those presented by Rodrik-Outmezguine are not only related to the dose but also tumor background. In their report they have used the BT474 breast cancer model which has a strong RTK "drive" via the erbB family and these receptors seem to be the target of the feedback. The tumor models that we have used are not notably erbB family RTK driven.

Across several of our models we showed a reduction in proximal biomarkers in response to the associated monotherapy and in the combination groups. Our group and others have previously shown that a phenotypic response to MEK inhibition does not accurately track with the extent of inhibition of ERK phosphorylation (36, 41, 49). As part of this study we wanted to use a MEK functional activation signature (41) to determine the functional output of the MEK pathway in response to the combination of selumetinib and AZD8055. We were able to show that a number of genes in the signature decreased in response to the combination of selumetinib and AZD8055, consistent with observations that selumetinib had also reduced levels of these genes. At the time points assayed in this study, one gene, *DUSP6*, was observed to change significantly in response to dual targeting of these agents in all 3 models tested. DUSP6 is a negative regulator of the MAPK family associated with cellular proliferation and differentiation (49). In addition the response of the gene signature output to AZD8055 did not seem to significantly change, suggesting that the increases in pERK we observed in response to AZD8055 (Figs. 1B and 3B) did not seem to effect MEK functional output, further highlighting that some caution is required when interpreting pERK data (36).

The PI3K/AKT/mTOR and MAPK pathways converge on the proapoptotic Bcl-2 homology 3 (BH3) family of proteins which regulate apoptosis (50). Mechanistically a consistent observation from our studies was an increase in apoptosis in the combination group compared with the single-agent treatment groups. In the 3 models analyzed pharmacodynamically (CaLu-6, HCT-116 and L004), there were increases in the downstream apoptotic effectors cleaved caspase 3 and/or cleaved PARP. The induction of apoptosis when the MAPK and PI3K/AKT/mTOR pathways are both inhibited has been frequently observed across a number of genetic subtypes (21, 43, 51). Furthermore, a number of *in vitro* studies have shown that increases in the proapoptotic protein Bim is observed following combination therapy (26, 52). In our studies we wanted to evaluate this mechanistic observation in our *in vivo* models. Here we have shown that in the CaLu-6 xenograft and L004 NSCLC explant models Bim levels were greater in the combination group than that of the monotherapy. In response to selumetinib and the combination treatment a dephosphorylation of Bim was seen, consistent with the mechanistic rationale of MEK pathway inhibition. Several *in vitro* studies have shown that in response to MEK inhibition alone or in

Published OnlineFirst January 23, 2012; DOI: 10.1158/0008-5472.CAN-11-1780

combination with PI3K/AKT/mTOR agents, that Bim, along with other BH3 proteins, mediates the observed apoptotic response (43, 52, 53). Therefore the observations in our studies suggest that Bim may be contributing to the apoptotic response.

Further studies *in vitro* have been able to dissect the effects of dual inhibition on the signaling of BH3 family proteins. A recent study in AML showed a decrease in Mcl-1 following combined treatment with the PI3K/AKT inhibitor perifosine and MEK inhibitors PD184352 or U0126 (52). In our tumor tissue we did assess Mcl-1 levels but did not detect any difference in any of the treatment groups compared with the controls (data not shown); this might reflect a cell type or time dependence for Mcl-1 modulation by MEK inhibition that is different from the effects of Bim.

In summary, we have presented a detailed preclinical evaluation, in human tumor xenograft and patient-derived tumor xenograft models with a range of genetic backgrounds, showing that the combination of selumetinib and AZD8055 is more effective than either agent alone. We have been able to present detailed phamacodynamic profiling showing that MEK functional outputs, as well as primary biomarkers, are modulated in response to the dual therapy. The use of several patient-derived tumor xenograft models has enabled us to monitor the combination of selumetinib and AZD8055 in tumor tissue considered to have a greater histologic and genetic heterogeneity than cell line–derived xenografts. Taken together the work presented here suggests that the combination of selumetinib and AZD8055 is a promising therapeutic strategy and warrants further preclinical and clinical investigation to determine an optimal setting for clinical testing.

Disclosure of Potential Conflicts of Interest

No potential conflicts of interest were disclosed.

Acknowledgments

The authors thank Jeremy Frith and members of the Cancer Disease Modelling Group (CDMG) at Alderley Park, the *in vivo* group at the ICC, Neil Gray and the Cancer IHC group at Alderley Park and the ICC.

Grant Support

All work was funded by AstraZeneca Pharmaceuticals.

The costs of publication of this article were defrayed in part by the payment of page charges. This article must therefore be hereby marked *advertisement* in accordance with 18 U.S.C. Section 1734 solely to indicate this fact.

Received May 24, 2011; revised December 19, 2011; accepted January 16, 2012; published OnlineFirst January 23, 2012.

References

1. Yoon S, Seger R. The extracellular signal-regulated kinase: multiple substrates regulate diverse cellular functions. Growth Factors 2006;24:21–44.
2. Sebolt-Leopold JS, Herrera R. Targeting the mitogen-activated protein kinase cascade to treat cancer. Nat Rev Cancer 2004;4:937–47.
3. Banerji U, Camidge DR, Verheul HM, Agarwal R, Sarker D, Kaye SB, et al. The first-in-human study of the hydrogen sulfate (Hyd-sulfate) capsule of the MEK1/2 inhibitor AZD6244 (ARRY-142886): a phase I open-label multicenter trial in patients with advanced cancer. Clin Cancer Res 2010;16:1613–23.
4. Infante JR, Fecher LA, Nallapareddy S, Gordon MS, Flaherty KT, Cox DS, et al. Safety and efficacy results from the first-in-human study of the oral MEK 1/2 inhibitor GSK1120212. J Clin Oncol 2010;28:2503.
5. Lorusso PM, Adjei AA, Varterasian M, Gadgeel S, Reid J, Mitchell DY, et al. Phase I and pharmacodynamic study of the oral MEK inhibitor CI-1040 in patients with advanced malignancies. J Clin Oncol 2005;23:5281–93.
6. Rinehart J, Adjei AA, Lorusso PM, Waterhouse D, Hecht JR, Natale RB, et al. Multicenter phase II study of the oral MEK inhibitor, CI-1040, in patients with advanced non-small-cell lung, breast, colon, and pancreatic cancer. J Clin Oncol 2004;22:4456–62.
7. Bast RC Jr, Hennessy B, Mills GB. The biology of ovarian cancer: new opportunities for translation. Nat Rev Cancer 2009;9:415–28.
8. Marsit CJ, Zheng S, Aldape K, Hinds PW, Nelson HH, Wiencke JK, et al. PTEN expression in non-small-cell lung cancer: evaluating its relation to tumor characteristics, allelic loss, and epigenetic alteration. Hum Pathol 2005;36:768–76.
9. Saal LH, Holm K, Maurer M, Memeo L, Su T, Wang X, et al. PIK3CA mutations correlate with hormone receptors, node metastasis, and ERBB2, and are mutually exclusive with PTEN loss in human breast carcinoma. Cancer Res 2005;65:2554–9.
10. Carretero J, Medina PP, Pio R, Montuenga LM, Sanchez-Cespedes M. Novel and natural knockout lung cancer cell lines for the LKB1/STK11 tumor suppressor gene. Oncogene 2004;23:4037–40.
11. Matsumoto S, Iwakawa R, Takahashi K, Kohno T, Nakanishi Y, Matsuno Y, et al. Prevalence and specificity of LKB1 genetic alterations in lung cancers. Oncogene 2007;26:5911–8.
12. Engelman JA. Targeting PI3K signalling in cancer: opportunities, challenges and limitations. Nat Rev Cancer 2009;9:550–62.
13. Guertin DA, Sabatini DM. Defining the role of mTOR in cancer. Cancer Cell 2007;12:9–22.
14. Chresta CM, Davies BR, Hickson I, Harding T, Cosulich S, Critchlow SE, et al. AZD8055 is a potent, selective, and orally bioavailable ATP-competitive mammalian target of rapamycin kinase inhibitor with *in vitro* and *in vivo* antitumor activity. Cancer Res 2010;70:288–98.
15. Feldman ME, Apsel B, Uotila A, Loewith R, Knight ZA, Ruggero D, et al. Active-site inhibitors of mTOR target rapamycin-resistant outputs of mTORC1 and mTORC2. PLoS Biol 2009;7:e38.
16. Thoreen CC, Kang SA, Chang JW, Liu Q, Zhang J, Gao Y, et al. An ATP-competitive mammalian target of rapamycin inhibitor reveals rapamycin-resistant functions of mTORC1. J Biol Chem 2009;284:8023–32.
17. O'Reilly KE, Rojo F, She QB, Solit D, Mills GB, Smith D, et al. mTOR inhibition induces upstream receptor tyrosine kinase signaling and activates Akt. Cancer Res 2006;66:1500–8.
18. http://www.fda.gov/AboutFDA/CentersOffices/OfficeofMedicalProductsandTobacco/CDER/ucm231967.htm.
19. Adjei AA, Cohen RB, Franklin W, Morris C, Wilson D, Molina JR, et al. Phase I pharmacokinetic and pharmacodynamic study of the oral, small-molecule mitogen-activated protein kinase kinase 1/2 inhibitor AZD6244 (ARRY-142886) in patients with advanced cancers. J Clin Oncol 2008;26:2139–46.
20. Atkins MB, Hidalgo M, Stadler WM, Logan TF, Dutcher JP, Hudes GR, et al. Randomized phase II study of multiple dose levels of CCI-779, a novel mammalian target of rapamycin kinase inhibitor, in patients with advanced refractory renal cell carcinoma. J Clin Oncol 2004;22:909–18.
21. Sos ML, Fischer S, Ullrich R, Peifer M, Heuckmann JM, Koker M, et al. Identifying genotype-dependent efficacy of single and combined PI3K- and MAPK-pathway inhibition in cancer. Proc Natl Acad Sci U S A 2009;106:18351–6.
22. Sun SY, Rosenberg LM, Wang X, Zhou Z, Yue P, Fu H, et al. Activation of Akt and eIF4E survival pathways by rapamycin-mediated mammalian target of rapamycin inhibition. Cancer Res 2005;65:7052–8.

Published OnlineFirst January 23, 2012; DOI: 10.1158/0008-5472.CAN-11-1780

23. Carracedo A, Ma L, Teruya-Feldstein J, Rojo F, Salmena L, Alimonti A, et al. Inhibition of mTORC1 leads to MAPK pathway activation through a PI3K-dependent feedback loop in human cancer. J Clin Invest 2008;118:3065–74.
24. Hoeflich KP, O'Brien C, Boyd Z, Cavet G, Guerrero S, Jung K, et al. *In vivo* antitumor activity of MEK and phosphatidylinositol 3-kinase inhibitors in basal-like breast cancer models. Clin Cancer Res 2009;15:4649–64.
25. Engelman JA, Chen L, Tan X, Crosby K, Guimaraes AR, Upadhyay R, et al. Effective use of PI3K and MEK inhibitors to treat mutant Kras G12D and PIK3CA H1047R murine lung cancers. Nat Med 2008;14:1351–6.
26. Kinkade CW, Castillo-Martin M, Puzio-Kuter A, Yan J, Foster TH, Gao H, et al. Targeting AKT/mTOR and ERK MAPK signaling inhibits hormone-refractory prostate cancer in a preclinical mouse model. J Clin Invest 2008;118:3051–64.
27. Legrier ME, Yang CP, Yan HG, Lopez-Barcons L, Keller SM, Perez-Soler R, et al. Targeting protein translation in human non small cell lung cancer via combined MEK and mammalian target of rapamycin suppression. Cancer Res 2007;67:11300–8.
28. Halilovic E, She QB, Ye Q, Pagliarini R, Sellers WR, Solit DB, et al. PIK3CA mutation uncouples tumor growth and cyclin D1 regulation from MEK/ERK and mutant KRAS signaling. Cancer Res 2010;70:6804–14.
29. Jaiswal BS, Janakiraman V, Kljavin NM, Eastham-Anderson J, Cupp JE, Liang Y, et al. Combined targeting of BRAF and CRAF or BRAF and PI3K effector pathways is required for efficacy in NRAS mutant tumors. PLoS One 2009;4:e5717.
30. She QB, Solit DB, Ye Q, O'Reilly KE, Lobo J, Rosen N. The BAD protein integrates survival signaling by EGFR/MAPK and PI3K/Akt kinase pathways in PTEN-deficient tumor cells. Cancer Cell 2005;8:287–97.
31. Bennouna J, Lang I, Valladares-Ayerbes M, Boer K, Adenis A, Escudero P, et al. A Phase II, open-label, randomised study to assess the efficacy and safety of the MEK1/2 inhibitor AZD6244 (ARRY-142886) versus capecitabine monotherapy in patients with colorectal cancer who have failed one or two prior chemotherapeutic regimens. Invest New Drugs 2010;29:1021–8.
32. Hainsworth JD, Cebotaru CL, Kanarev V, Ciuleanu TE, Damyanov D, Stella P, et al. A phase II, open-label, randomized study to assess the efficacy and safety of AZD6244 (ARRY-142886) versus pemetrexed in patients with non-small cell lung cancer who have failed one or two prior chemotherapeutic regimens. J Thorac Oncol 2010;5:1630–6.
33. Davies BR, Logie A, McKay JS, Martin P, Steele S, Jenkins R, et al. AZD6244 (ARRY-142886), a potent inhibitor of mitogen-activated protein kinase/extracellular signal-regulated kinase kinase 1/2 kinases: mechanism of action *in vivo*, pharmacokinetic/pharmacodynamic relationship, and potential for combination in preclinical models. Mol Cancer Ther 2007;6:2209–19.
34. Holt SV, Wyspianska B, Randall KJ, James D, Foster JR, Wilkinson RW. The development of an immunohistochemical method to detect the autophagy-associated protein LC3-II in human tumor xenografts. Toxicol Pathol 2011;39:516–23.
35. Wilkinson RW, Odedra R, Heaton SP, Wedge SR, Keen NJ, Crafter C, et al. AZD1152, a selective inhibitor of Aurora B kinase, inhibits human tumor xenograft growth by inducing apoptosis. Clin Cancer Res 2007;13:3682–8.
36. Gopal YN, Deng W, Woodman SE, Komurov K, Ram P, Smith PD, et al. Basal and treatment-induced activation of AKT mediates resistance to cell death by AZD6244 (ARRY-142886) in Braf-mutant human cutaneous melanoma cells. Cancer Res 2010;70:8736–47.
37. Mirzoeva OK, Das D, Heiser LM, Bhattacharya S, Siwak D, Gendelman R, et al. Basal subtype and MAPK/ERK kinase (MEK)-phosphoinositide 3-kinase feedback signaling determine susceptibility of breast cancer cells to MEK inhibition. Cancer Res 2009;69:565–72.
38. Ley R, Balmanno K, Hadfield K, Weston C, Cook SJ. Activation of the ERK1/2 signaling pathway promotes phosphorylation and proteasome-dependent degradation of the BH3-only protein, Bim. J Biol Chem 2003;278:18811–6.
39. Luciano F, Jacquel A, Colosetti P, Herrant M, Cagnol S, Pages G, et al. Phosphorylation of Bim-EL by Erk1/2 on serine 69 promotes its degradation via the proteasome pathway and regulates its proapoptotic function. Oncogene 2003;22:6785–93.
40. Rubio-Viqueira B, Hidalgo M. Direct *in vivo* xenograft tumor model for predicting chemotherapeutic drug response in cancer patients. Clin Pharmacol Ther 2009;85:217–21.
41. Dry JR, Pavey S, Pratilas CA, Harbron C, Runswick S, Hodgson D, et al. Transcriptional pathway signatures predict MEK addiction and response to selumetinib (AZD6244). Cancer Res 2010;70:2264–73.
42. Weinstein IB, Joe A. Oncogene addiction. Cancer Res 2008;68:3077–80.
43. Meng J, Fang B, Liao Y, Chresta CM, Smith PD, Roth JA. Apoptosis induction by MEK inhibition in human lung cancer cells is mediated by Bim. PLoS One 2010;5:e13026.
44. Sarbassov DD, Ali SM, Kim DH, Guertin DA, Latek RR, Erdjument-Bromage H, et al. Rictor, a novel binding partner of mTOR, defines a rapamycin-insensitive and raptor-independent pathway that regulates the cytoskeleton. Curr Biol 2004;14:1296–302.
45. Sarbassov DD, Ali SM, Sengupta S, Sheen JH, Hsu PP, Bagley AF, et al. Prolonged rapamycin treatment inhibits mTORC2 assembly and Akt/PKB. Mol Cell 2006;22:159–68.
46. Alessi DR, Caudwell FB, Andjelkovic M, Hemmings BA, Cohen P. Molecular basis for the substrate specificity of protein kinase B; comparison with MAPKAP kinase-1 and p70 S6 kinase. FEBS Lett 1996;399:333–8.
47. Rodrik-Outmezguine VS, Chandarlapaty S, Pagano NC, Poulikakos PI, Scaltriti M, Moskatel E, et al. mTOR kinase inhibition causes feedback-dependent biphasic regulation of AKT signaling. Cancer Discov 2011;1:248–59.
48. Naing A, Aghajanian C, Raymond E, Kurzrock R, Blanco M, Oelmann E, et al. First results from a phase I trial of AZD8055, a dual mTORC1 and mTORC2 inhibitor. Mol Cancer Ther 2011;10; (Meeting Abstract Supplement) A168.
49. Pratilas CA, Taylor BS, Ye Q, Viale A, Sander C, Solit DB, et al. (V600E) BRAF is associated with disabled feedback inhibition of RAF-MEK signaling and elevated transcriptional output of the pathway. Proc Natl Acad Sci U S A 2009;106:4519–24.
50. McCubrey JA, Steelman LS, Abrams SL, Lee JT, Chang F, Bertrand FE, et al. Roles of the RAF/MEK/ERK and PI3K/PTEN/AKT pathways in malignant transformation and drug resistance. Adv Enzyme Regul 2006;46:249–79.
51. Lasithiotakis KG, Sinnberg TW, Schittek B, Flaherty KT, Kulms D, Maczey E, et al. Combined inhibition of MAPK and mTOR signaling inhibits growth, induces cell death, and abrogates invasive growth of melanoma cells. J Invest Dermatol 2008;128:2013–23.
52. Rahmani M, Anderson A, Habibi JR, Crabtree TR, Mayo M, Harada H, et al. The BH3-only protein Bim plays a critical role in leukemia cell death triggered by concomitant inhibition of the PI3K/Akt and MEK/ERK1/2 pathways. Blood 2009;114:4507–16.
53. Cragg MS, Jansen ES, Cook M, Harris C, Strasser A, Scott CL. Treatment of B-RAF mutant human tumor cells with a MEK inhibitor requires Bim and is enhanced by a BH3 mimetic. JCI 2008;118:3651–9.